Biomedical Engineering Letters (2020) 10:63–81
https://doi.org/10.1007/s13534-019-00120-0

REVIEW ARTICLE

Non-radiative healing assessment techniques for fractured long bones and osseointegrated implant

S. Lu[1] · B. S. Vien[1] · M. Russ[2,3] · M. Fitzgerald[2,3] · W. K. Chiu[1]

Received: 3 May 2019 / Revised: 4 July 2019 / Accepted: 12 July 2019 / Published online: 26 July 2019

Abstract
The paper provides an overview of the fracture healing process of long bones, a review of work that proposed appropriate physical parameters for the assessment of healing and highlights some recent work that reported on the development of non-radiative technique for healing assessment. An overview of the development and monitoring of osseointegration for trans-femoral osseointegrated implant is also presented. The state of healing of a fractured long bone and the stability of osseointegrated implants can be seen as engineering structural components where the mechanical properties are restored to facilitate their desired function. To this end, this paper describes non-radiative techniques that are useful for healing assessment and the stability assessment of osseointegrated implants. The achievement of non-radiative quantitative assessment methodologies to determine the state of healing of fractured long bones and to assess the stability of osseointegrated implant will shorten the patient's rehabilitation time, allowing earlier mobility and return to normal activities. Recent work on the development of assessment techniques supported by the Office of Naval Research as part of the Monitoring of Osseointegrated Implant Prosthesis program is highlighted.

Keywords Fracture healing · Acoustic emission · Vibrational analysis · Quantitative ultrasound · Osseointegration

1 Introduction

The current techniques for assessing the state of healing of fixated fractured long bones include X-ray, Computed Tomography (CT), and manual manipulation. Unfortunately, these methods have significant drawbacks for the patient, primarily exposure to radiation, and, in most cases, provide images that are suitable for qualitative assessment of the state of healing of a fracture. In addition, these are qualitative assessments where their accuracy depends on the surgeon's experience (Claes et al. [1]; Morshed et al. [2]). A robust diagnostic tool to quantitatively evaluate the state of fracture healing will improve the patient's care. The ability to define completed fracture healing and the identification of delayed union will greatly assist with the management of the fracture. One of the aims of this paper is to provide a review of the work done in the development of a non-radiative quantitative assessment technique for the healing assessment of fractured long bones, especially the femur and tibia. Non-radiographic quantitative assessment techniques can complement existing radiographic techniques. A reduction in the reliance on X-ray and CT will limit the exposure to harmful radiation. The paper provides an overview of the fracture healing process, work that proposed appropriate physical parameters for the assessment of healing and highlighted some recent work that reported on the development of three non-radiative techniques for healing assessment. Osseointegration technique was first applied to the area of

✉ S. Lu
shouxun.lu@monash.edu

B. S. Vien
ben.vien@monash.edu

M. Russ
M.Russ@alfred.org.au

M. Fitzgerald
M.Fitzgerald@alfred.org.au

W. K. Chiu
wing.kong.chiu@monash.edu

[1] Department of Mechanical & Aerospace Engineering, Monash University, Wellington Rd, Clayton, VIC 3800, Australia

[2] The Alfred Hospital, 55 Commercial Road, Melbourne, VIC 3004, Australia

[3] National Trauma Research Institute, 89 Commercial Road, Melbourne, VIC 3004, Australia

dentistry, and then it was extended to orthopaedics and limb amputees pioneered by Rickard Bårenmark. Titanium and its alloys are commonly used as implants due to their excellent biocompatibility and superior mechanical properties. Osseointegration prosthesis has an advantage in improving mobility and quality of life for the amputee compared to the socket prosthesis [3, 4]. Nevertheless, the osseointegration process is complex, and many factors influence the formation of the bone at the implant surface. Since implant stability is a primary concern [5–7], this paper presents a review of the quantitative stability assessment techniques for osseointegrated implants. Indeed, the monitoring and assessment techniques that are proposed for healing assessment can also be extended for assessing the stability of osseointegrated implants. The paper describes recent development in the design of customisable osseointegrated implant where sensing elements can be integrated into this device for assessing the degree of osseointegration or the lack of it.

2 Healing process

2.1 Fracture healing process

Bone fracture healing is a highly complex and dynamic process which gradually recovers its biological function and mechanical properties. This process can be described in four basic steps: inflammation, cellular proliferation, differentiation, and remodelling [8]. During the inflammation step, the injury on the blood vessel caused by bone fracture leads to regional hypo-perfusion in neighbour area. The coagulation cascade is initiated by the exposure of vascular endothelium (vessel interior surface) and intravascular cells, leading to the formation of haematoma, which is abundant in platelets and macrophages. The inflammatory mediators release from haematoma trigger an inflammatory response, which consists of an increase in blood flow, vascular permeability, and inflammatory cell migration.

With respect to cellular proliferation and differentiation, the healing process is largely dependent on the mechanical environment. There are two types of healing, direct and indirect fracture healing [9]. Direct healing does not involve inter-fragmentary gap and rigid fixation, which can only be achieved by open reduction and internal fixation surgery. The healing is achieved via the reconstruction of the anatomical lamellar bone, the Haversian canals (a microstructure include the path for nerves and blood) and blood vessels. Indirect healing relates to treatments that allow inter-fragmentary motion and rigid internal or external fixation. During indirect healing, the primitive mesenchymal stem cells drift into the fracture site and differentiate into a cell with osteogenic potential, which leads to the formation of tissue in the fracture site. The tissue provides a connection between fracture ends known as a callus. With the mineralization process known as ossification, the soft callus is converted into woven bone. After months of remodelling, the woven bone is replaced by lamellar bone, which has highly ordered microstructure.

2.2 The relationship between the fracture healing process and bone stiffness/strength

Mora-Macías et al. [10] evaluated quantifiable biological parameters relative to mechanical parameters during the ossification process. They concluded that during the ossification, the axial stiffness (defined as the ratio of load and the corresponding displacement) of the callus increased exponentially respect to the healing time. When the volume of callus reached 80% of the maximum volume, callus stiffness was below 10% of that of the healthy bone. The stiffness was observed to increase rapidly after the callus achieved maximum volume and the bone recovered its load bearing capability. Similar results of animal bone were reported in Leong et al. [11, 12]. Dwyer et al. [13] reported similar behaviour with human bone during the ossification process. In the view of mechanics, this ‘stiffness” can be related to the elastic modulus of the bone.

Chehade et al. [14] reported on the correlation between bending stiffness and strength during the healing fracture by using the four-point bending mechanical test. A total of 40 skeletally mature sheep were divided into 5 groups and culled at 2, 4, 6, 8 and 10 weeks. A transverse osteotomy was applied at the mid-shaft of the left tibia. The formation of callus was determined from the observation of the tibia that was culled at 2, 4, 6, 8 and 10 weeks. During this process, at the initial stages of the fracture healing, they reported a correlation between the stiffness and strength. However, during the remodelling phase, the further increase in strength is accompanied by a small change in stiffness. They attributed this to the organized orientation and mineralization of the collagen fibres in callus that lead to an increasing amount of lamellar bone. According to their experimental data, there was no longer a clear correlation between stiffness and strength once the stiffness of callus reached approximately 65% of that of the healthy bone. Therefore, the stiffness could only determined the baseline of the strength. This finding is similar to that reported in Mora-Macías et al. [10] who stated that the bone was capable of load bearing (high strength) when the stiffness was still relatively low. A similar correlation was also reported in human bone Claes et al. [1], and Dwyer et al. [13]. These results suggest that “stiffness” may be a suitable parameter to assess the state of healing.

3 Fracture fixation techniques

3.1 External fixation

External fixation is a method that aims to provide sufficient stability of fractured bones by utilizing a percutaneously external device. The structure consists of percutaneous pins or wires, claps, sidebars or rings and struts. The most common type of external fixator is a combination of the pins and bars. Pins are inserted into the bone and sidebars are connected to pins through the pin clamp (see Fig. 1). The stiffness or rigidity of the whole construct can be enhanced with the deployment of the pins and sidebars. The external fixation is suitable for higher-energy polytrauma patients who suffer soft tissue injuries or open wounds. External fixation has a relatively low risk of infection and better pain control. Patients with external fixation have better access to wound care and less risk of bone non-unions. In addition, the external pin clamp structure allows the adjustment of the construct, which facilitates fracture alignment and realignment [15]. However, the insertion of pins creates a communicating tract between skin and bone, which may potentially increase the chance of soft tissue infection. In addition, the external device will limit patient mobility in normal daily life [16].

3.2 Internal fixation

3.2.1 Intramedullary nail

Intramedullary nail (IM nail) refers to a clinical method of internal fixation for treating long bone fractures. IM nail consists of a cylindrical metal tube, which inserted into either proximal or distal end of the bone and lock in position via interlocking screws (see Fig. 2). These locking screws are fastened onto the cortical bone. The installed IM nail across the fracture site facilitates the transfer of rotational, compressive, and bending forces across the fracture site while preserving the anatomic alignment to induce bone union [17]. The bone is capable of enduring early loading during the fracture healing because of the stable internal fixation provided by IM nail [18]. Compared to the external fixation, intramedullary nail reduces the risk of pin tract sepsis [16]. However, the application of IM nail is limited because of the high risk of infection and local or systemic complications [19].

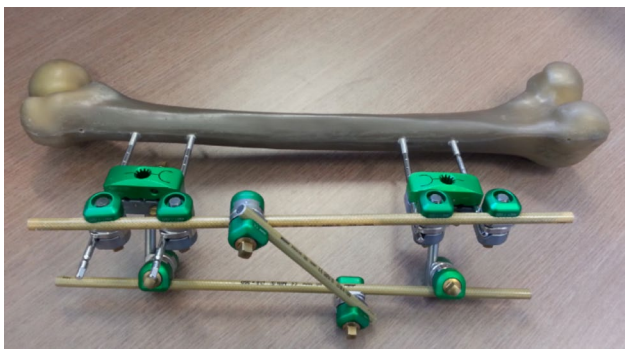

Fig. 1 Femur fixated with an external fixation

Fig. 2 X-ray scan of the patient with IM nail

3.2.2 Compression plate

There are two kinds of compression plate: locking compression plates (LCP) and dynamic compressional plate (DCP). DCP is also known as conventional plating which provides stability of the fracture site by the frictional force between the plate and bone (see Fig. 3). However, the plate is compressed directly onto the bone, which may cause

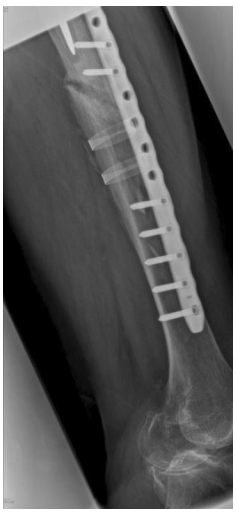

Fig. 3 X-ray scan of the patient with DCP

blood supply disturbance [20]. LCP, which has threaded holes, is a modified version of DCP. Therefore, either non-locking screws or locked screws can be utilised on LCP. With the mesh on the screw thread and thread hole, LCP allows the load transmission without compressing onto the bone, which enhances the blood supply compared to DCP [21]. However, compared to the intramedullary nail, early load bearing is forbidden for patients with a compression plate. In addition, due to the high stiffness of the plate, a compression plate may delay callus formation and induce bone resorption [22].

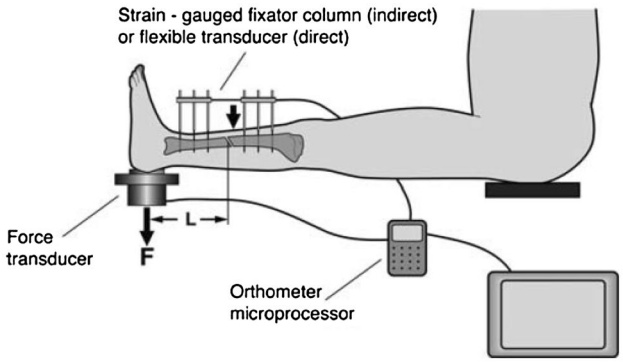

Fig. 4 Fracture stiffness measurement after removal of the external fixator [1]

4 Techniques for monitoring fracture healing

There are two clinically available techniques in evaluating the degree of fracture healing of long bones are radiographical technique and biomechanical testing. Radiography is a common methodology in non-destructive evaluation in engineering structural assessments. In contrast to the quantitative biomechanical testing, the radiographic image allows the physician to inspect the alignment of the fracture site qualitatively [23]. It is also known that the three-dimensional computed tomography radiographic technique can provide a quantitative assessment of the state of healing. This method can provide a quantitative assessment of the callus volume and the average mineral density [24], thereby allowing for the estimation of Young modulus of the bone. In addition, Sigurdsen et al. [25] reported a correlation between the bending strength and the volumetric bone mineral density around the fracture site in the early phase of fracture healing [25]. However, the high radiation dosage limits regular CT usage for healing assessment [2].

Biomechanical techniques for healing assessment is a form of non-radiative methodologies for healing assessment is an on-going research area. Biomechanical testing includes direct and indirect methods [1]. Direct testing refers to the evaluation of the callus stiffness by measuring the deflection of the healing bone under a certain loading. The leg is rested in the horizontal position and loaded by weight or manually at the distal end, producing a bending moment. A transducer is connected to the pin clamp to measure the deformation of the long bone [1]. Indirect testing evaluates the stiffness of callus through the decrease in the loading taken by the external fixation with strain gauges attached to the sidebar [1]. The orthometer microprocessor was used to measure the deflection of bone under loading as illustrated in Fig. 4. In general, the deformation along the longitudinal axis is the key parameter in determining the stage of fracture healing in clinical applications. However, the most significant drawback is its applicability to patients with external fixations. In this case, the external fixation has to be disassembled for each stiffness measurement, therefore increasing the risk of re-fracture and misalignment especially for the femur in the early phase of healing. Although the engineering principles are sound, the clinical application for these forms of testing is limited (Claes et al. [1]; Morshed et al. [2]). The other non-radiative healing assessment techniques that have been reportedly investigated on include the following:

4.1 Acoustic emission

Acoustic emission (AE) refers to transient elastic waves, which occur when strain energy is suddenly released with the micro-damage formation of a structure [26]. The space shuttle Columbia disaster upon re-entry, leading to disintegration of the spacecraft and the loss of seven crew members, has served to focus worldwide attention on the requirement for effective structural health monitoring (SHM) techniques as a key enabling technology for future space exploration and space technologies [27, 28]. In particular, acoustic emission (AE) sensors have been deployed and evaluated for impact detection on subsequent shuttle flights AE has been widely used as a SHM method in the industry. AE testing has been categorized as a non-invasive method since the structural integrity is preserved after testing. The elastic waves are detected and the source is localised by embedded piezoelectric discs or transducers. In the biomechanical field, the AE examination was firstly used in detecting micro-fractures, which were not clearly diagnosed by conventional X-ray Hirasawa et al. [29] Furthermore, acoustic emission was applied to predict the bone mechanical properties changes due to fatigue (Shrivastava et al. [30]; Agcaoglu et al. [31]).

In 2001, Watanabe et al. [32] conducted an experiment on 120 male rats to investigate the relationship between the load and the mechanical strength of the callus. In this experiment, rats were treated with femur osteotomy, generating 2 mm gaps in the mid-shaft on the right femur. A specially

designed stainless-steel nail with four interlocking needles was fixed at the gap to prevent shortening and rotation at the osteotomy site. The rats were euthanized to determine callus tensile strength and torsional strength at 4, 6, 8, and 12 weeks after surgery. The specimens were loaded with tensile force and torque respectively to failure to record the AE signal. Based on the result, they found that forces and torques for initiation of AE presented a clear and positive linear correlation with tensile strength and maximum torque (see Fig. 5). This method was suitable for the patients treated with external fixation since the signal should be easily detected through the pins. In addition, the surgeon could re-install the fixation instantly to continue the treatment, even though micro-damage occurred when the AE signal was detected. From these reasons, they deemed it possible to used AE testing as a fracture healing monitoring method. However, AE signals of this experiment were retrieved under in vitro condition. Therefore, this method was currently shown to be only suitable for the patients treated with external fixation, which the AE signals were detected through pins or screws.

Based on Watanabe's results, Hirasawa [29] proposed an investigation on monitoring the fracture healing by acoustic emission for 35 patients with 39 long bones treated with external fixation. In their experiment, two wide-band piezoelectric transducers were attached to the half-pins or transfixation wires, which were held by a specially designed holder after removal of the external bridge. Acoustic emission signals were monitored during application of a step-increased axial load at the rate of 5 kg per 5 s to callus. Based on the results of the AE testing, 97% of patients removed their external fixation when no acoustic emission signal was detected on full weight bearing load. All except one patient endured a re-fracture in the callus area after removal. The results suggested acoustic emission techniques could be employed to assess fracture healing. According to their result, 46% of fracture could not be interpreted as a "healed" by radiographic diagnosis when the fracture is assessed as being healed using acoustic emission. This provided an impetus for the quantitative assessment by methods apart from radiographic ones. In their work, only the axial compression loading was considered, which was not sufficient to determine the bone union [29]. Other parameters such as torsional or bending stiffness should be included in AE examination. Moreover, to ensure the safety of patients, the AE measurement was applied when two of five physicians regard as fracture healing completed (union). Authors suggested that the current AE method could only be used as complementary to radiography result. Even though there have been several research conducted on the bones obtained from the cadavers or on the volunteers, the detection of AE signal in current method means the micro-damage to the callus had occurred, limiting the application of AE in the early phase of healing. A further investigation of non-destructive AE evaluation in fracture healing and a number of investigation on the reliability and accuracy might be the future target.

4.2 Quantitative ultrasound

4.2.1 First-arriving signal velocity measurement

Quantitative ultrasound (QUS) has been previously employed as a tool to monitor structural components. The first application of the ultrasound velocity measurement which is also known as First-arriving signal (FAS) velocity measurement on assessing fracture healing was investigated by Siegel et al. [33]. The animal [34] and clinical [35] studies demonstrated that the fracture site was capable of full-weight loading when the velocity of ultrasound achieved 80% that of intact bone. FAS relies on the axial transmission of the propagating ultrasound, refer to Fig. 6. The change

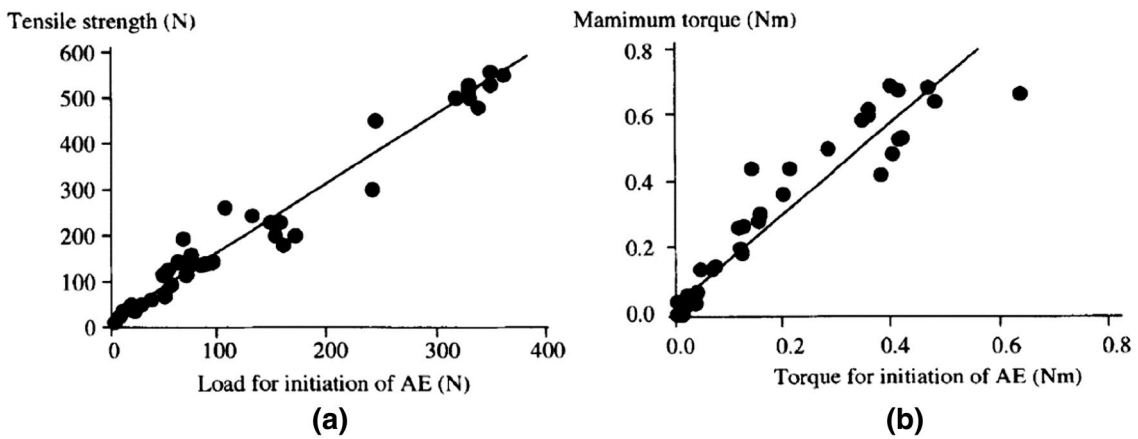

Fig. 5 Relationship: **a** the load for initiation of AE and tensile strength, **b** the torque for initation of AE and torsional mechanical property [32]

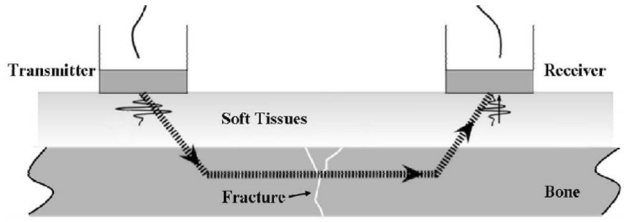

Fig. 6 Quantitative ultrasound of fracture healing in the long bone [33]

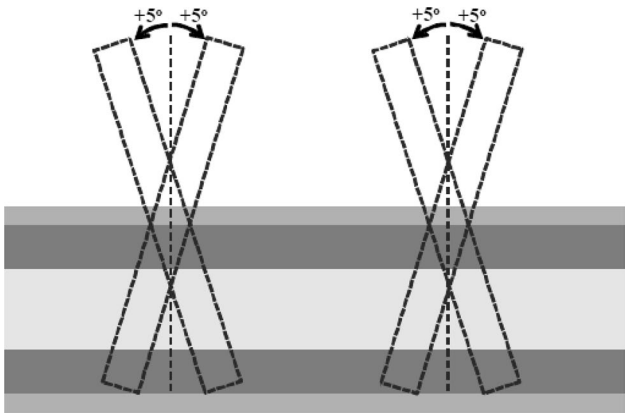

Fig. 7 The ± 5° angles of pin inclination [36]

in ultrasonic wave velocity caused by the difference in the material properties of callus and cortical bone when ultrasound passes through the fracture site is used as the primary parameter for healing assessment. By comparing the velocity value obtained from contra-lateral intact bone, the fracture healing processing can be quantitatively measured [33]. For percutaneous application, the ultrasound, which is injected through a transmitter attached on the skin, propagated along the bone, passes through the fracture site and is detected by the receiver. For trans-osseous method, the transducers are surgically implanted into fracture region and in contact with the periosteum. The typical frequency of the transmitter is in the range from 0.25 to 2.5 MHz. The velocity of the ultrasound is defined as the ratio of the longitudinal distance that ultrasound travelled to the transit time of the first-arriving signal.

In a 2D bone–plate simulation, Vavva et al. [36] validated the capability of attaching transducers to the external fixation pin to evaluate the fracture healing. Moreover, they also investigated the effects of the inclination of the pin on its ability to improve the FAS assessment technique. In their experiment setup, a 1 MHz ultrasonic wave was induced to ensure there is no guided wave emission. In addition, they added a 3 mm thick layer of blood on each side of the plate to simulate the overlying soft tissue. The external fixation pins were allowed to lean ± 5° from the vertical axis, refer to Fig. 7. The inclination of pins was evaluated through five different combinations of the pins' insertion angle. The result of the experiment demonstrated that the wave velocity transmitted through the stainless steel pins was higher than that in the bone which leads to a notable increase in the measured velocity compared to the result of percutaneous and trans-osseous methods (P&TM). In addition, the velocity change caused by the healing process was difficult to identify because of the significant increase in the wave velocity, leading to a reduction in the sensitivity for assessing and detecting fracture healing. FAS velocity showed a similar correlation with P&TM as healing progressed. Nevertheless, the inclination of pins had a minor effect on the correlation. The significant advantage over P&TM was the overlying tissue had no effect on FAS velocity measurement. In spite of the advantages, the accuracy of this method was limited by the high attenuation caused by signal reflection at the bone–pin interface. Malizos et al. [37] conducted an experimental study on 40 skeletally mature sheep with a transverse osteotomy at mid-shaft. The external fixations were utilised to provide stability. A telemedicine system, which consisted of a pair of implantable transducers, which emitted ultrasound with a frequency of 1 MHz, and a control module for data collecting and power supply purposes, was employed as a tool to monitor fracture healing. They also demonstrated that the FAS velocity decreased for a certain time after which the velocity has reached the value of intact bone. Protopappas et al. [38] showed a similar correlation between FAS velocity and post-operative time. However, the result provided by Vavva et al. [36] showed that the FAS velocity continuously increases during the healing process.

4.2.2 Guided wave application

Guided wave (GW) propagation has demonstrated promising potential for structural integrity monitoring due to its rapid area inspection with minimal attenuation. Dispersion curve is often determined to identify the wave modes and its higher orders. In practice, the wave mode is often denoted by a letter and a number identifying its mode type and order, i.e. S1—first order symmetric wave mode and A0—fundamental antisymmetric wave mode. Previous studies have employed GW to assess bone structures using FAS method [38, 39]. In using QUS technique, it is reported that the geometric condition along the transmission path may affect the ultrasound transmission. When the wavelength is smaller or similar to the thickness of cortical bone, the ultrasound wave propagates along the subsurface of bone at the bulk wave frequency. This means that the FAS velocity only shows ostensible information of the periosteal bone region. When the wavelength is larger than the cortical bone thickness, the guided waves, which are enhanced by the cylindrical shape of the bone, propagates through the bone and are dispersive.

With healing progressing, there is less energy dispersed to the surrounding soft tissue through the fracture site. This will lead to an energy increase for certain wave mode [38].

In the research reported by Protopappas et al. [38], they utilised the 2D intact bone plate model to investigate the effects of the callus properties and geometry on the dispersion characteristics of the guided wave modes on the bone. Subsequently, they carried an ex vivo experiment on the intact tibia with two transducers attached to bone surface perpendicularly, to show the applicability of GW. Two GWs with frequencies of 500 kHz and 1 MHz, which result in two wavelengths (8 mm and 4 mm respectively) that are larger than the plate thickness, were used in this research. The dominant wave modes at 1 MHz excitation were the S2 and A3 Lamb modes and at 500 kHz excitation, the dominant wave modes were S2 and S0 modes. According to the result, the FAS velocity relationship could not identify changes of the callus geometry, but it is sensitive to the stiffness change as the healing progressed. However, the time–frequency analysis showed an increased in the S2 mode along with the consolidation of callus and when Young's modulus of callus was less than 50% that of healthy bone. This method could enhance the FAS velocity measurement's viability and accuracy for fracture healing assessment. Nevertheless, the experiment on the real bone revealed that the ultrasonic energy would be dissipated into surrounding soft tissue and bone marrow, produced inaccurate and less reliable results [38].

4.3 Vibrational response

Works are on-going in developing the use of mechanical vibration as a fundamental principle for monitoring bone assessment [40–43]. The variation in the vibration characteristic such as resonant frequencies indicate the change in mechanical properties during the fracture healing [41]. Current research in this area mainly focus on long bones such as femur and tibia.

The first application, called auscultatory percussion, consists of an excitation source, generally, a micro-hammer or a diapason, taped on the distal end and a stethoscope at the opposite end, worked as a detector. The decrease in the volume and pitch revealed the bone fracture. Even though this method is non-invasive, it is unable to provide a quantitative measurement on fracture condition [40, 41]. Recently, more advanced vibration-based techniques have been developed. In previous papers, based on the in vivo and ex vivo test [23, 42, 43], researchers had already shown that the resonance frequency is a potential quantitative parameter for monitoring fracture healing process even with the influence of the soft tissue on the vibrational response. Alizad et al. [41] applied radiation force to induce vibration remotely within the frequency range of 0–10 kHz in the rat femur. The results showed that the resonant frequency in the femur showed an increasing trend with healing progressed.

4.3.1 Vibration response with external fixation

In the work funded by the United States Office of Naval Research (ONR), Ong et al. [44] indicated that there is a strong dependence of dynamic response on structural properties of a given construct. In the recent research funded by ONR, Ong et al. [44, 45] proposed a concept of integrating the sensing elements into external fixation to monitor fracture healing remotely. In their research [44], the potential of locating sensors on the external fixation and the appropriate frequency range were conceptualised using a series finite element analysis. This is then substantiated with a series of experimental study. Ong et al. [44] reported that the lower modes are dominated by the deformation of the external fixation and are insensitive to the bone structural change. In the frequency bandwidth between 200 and 400 Hz, these higher order modes were sensitive to the mechanical properties changes in the fracture region (see Fig. 8).

The change in the stiffness was depicted by the shift of the resonant behaviour. Ong et al. [44] also reported that the choice of location of the sensor elements and the drive point would affect the sensitivity of the healing assessment capability. However, the potential of using the pins of the external fixators to facilitate the excitation and the measurement of the corresponding dynamic response is clearly demonstrated. This finding was supported by Mattei et al. [40, 46] who also demonstrated signal damping, caused by soft tissue around the bone, could be reduced by using pins as a path for excitation and measurement.

The effects of soft-tissue on the dynamic response of a long bone is well known. This is known to impair the ability in using dynamic-based assessment techniques for healing assessment. As an example, Bediz et al. [43] reported that the mass loading, caused by soft tissue, decreased the resonant frequency of a long bone. It is worth noting that Ong et al. [45] also reported on work, which funded by ONR done to investigate the influence of the mass damping due to the surrounding soft tissue. In their work, the epoxy was applied at the fracture site to simulate the fracture healing process [40–42, 44, 45, 47]. These works reported on experiments performed using artificial composite bone specimen made from short fibre filled epoxy. The specimens were osteotomised to simulate fracture. Epoxy with long curing time (30 min) was used applied to the fractured region and to simulate healing. They introduced the concept of a healing index, which is computed from the dynamic response of the construct, and the rate of change of the healing index with respect to time HI_t, to simultaneously assist in evaluating different healing stages (Eq. 1).

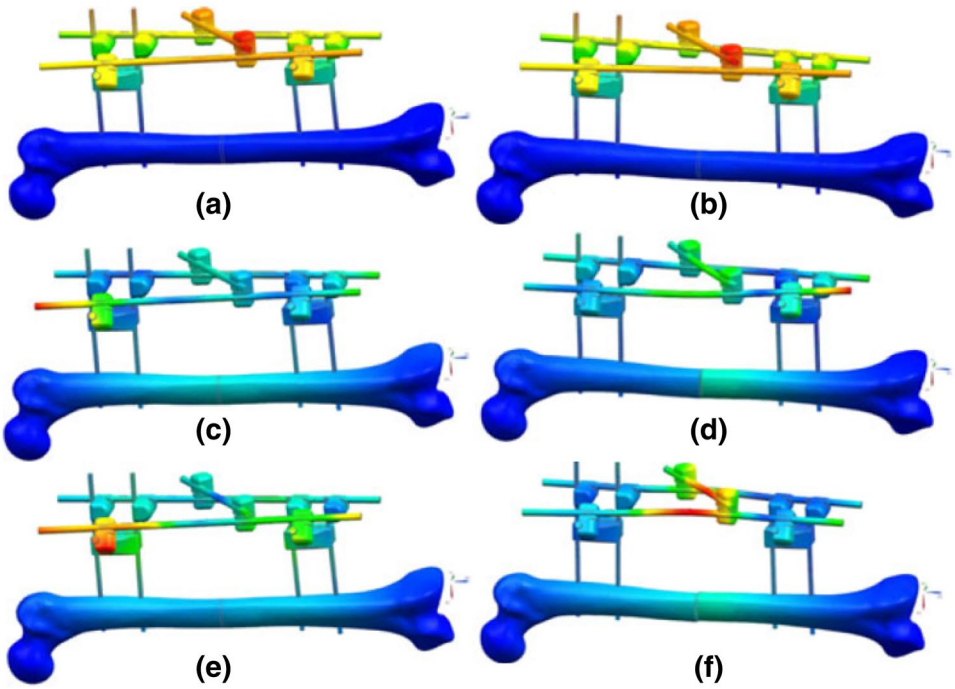

Fig. 8 Mode shapes. **a** No damage, Mode 1, 48 Hz. **b** Fractured, Mode 1, 48 Hz. **c** No damage, Mode 6, 283 Hz. **d** Fractured, Mode 8, 284 Hz. **e** No damage, Mode 8, 335 Hz. **f** Fractured, Mode 9, 328 Hz [45]

$$
\begin{aligned}
TF(fi) &= \frac{V_{input\ force}(fi)}{V_{PVDF}(fi)} \\
TF_{windowed}(fi) &= \int_{fi}^{fi+10} \left| TF_{t=xmin}(fi) - TF_{t=0\,\min(fi)} \right| df \\
Healing\ index &= \sum TF_{windowed}(fi) \\
HI_t &= \frac{d}{dt}(Healing\ index)
\end{aligned}
\tag{1}
$$

where $V_{input\ force}(fi)$ is voltage in the frequency domain obtained from force input; $V_{PVDF}(fi)$ is voltage in frequency domain obtained from polyvinylidene fluoride (PVDF) film sensor; $TF(fi)$ is the transfer function between force input and sensor response; $TF_{windowed}(fi)$ is the windowed average function obtained 10 Hz window; HI_t is differentiation of the healing index relative to time.

For a bone specimen without modelling clay (Ong et al. [45]), the frequency response measured with simulated

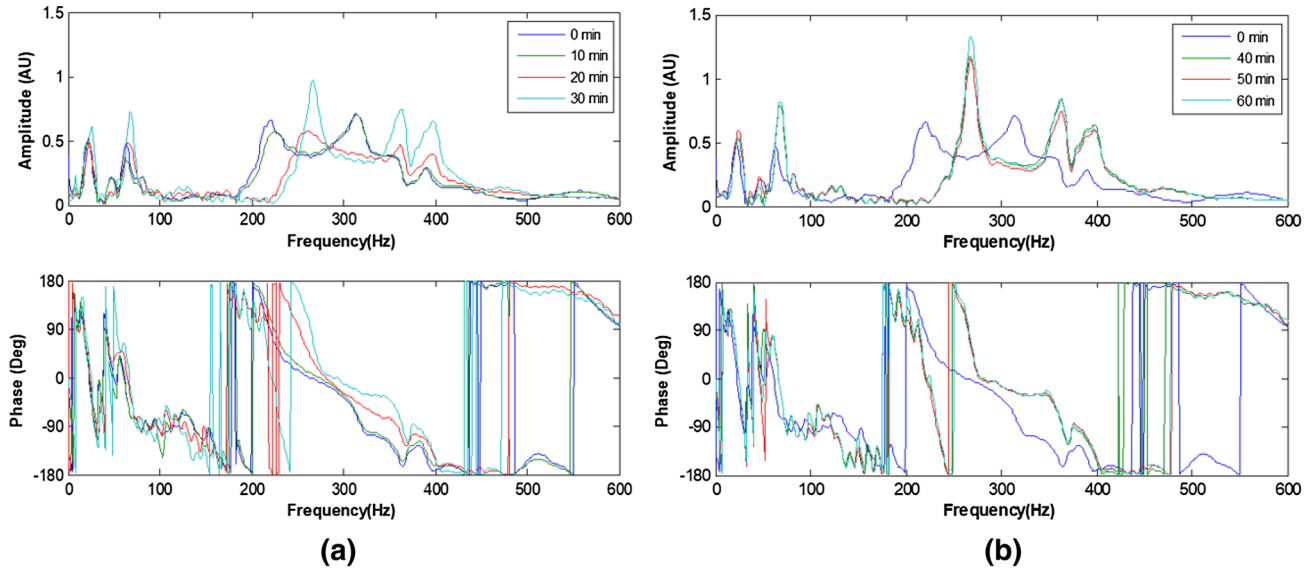

Fig. 9 Development of frequency response function resulting from simulated healing (30 min epoxy) **a** 0–30 min; **b** 40–60 min [45]

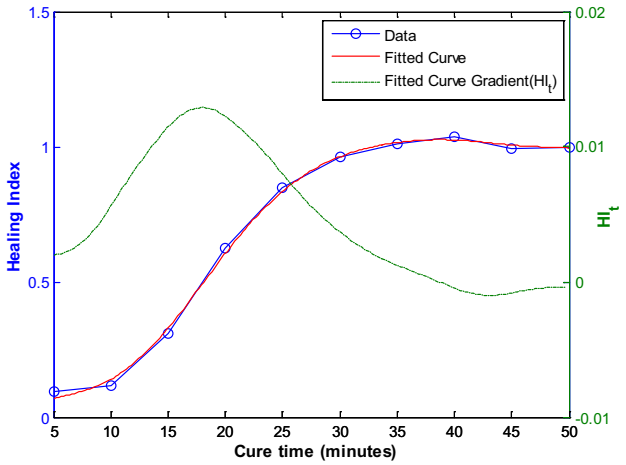

Fig. 10 Healing index calculated (without mass loading) [45]

healing is shown in Fig. 9. The shift in the resonant frequency as healing progressed is evident. The healing index is calculated from the spectra responses are shown in Fig. 10. These results show that the dynamic response of the construct is sensitive to the state of healing of the fractured region.

The experiments were repeated with the femur wrapped with highly dense and soft plasticine to simulate soft tissue. The resulting spectra response as a function of the healing time is shown in Fig. 11. Although the effects of mass loading are visible, the effects of healing on the spectra response is still discernible. The calculated healing index as illustrated in Fig. 12 and its time-derivative highlighted the viability of vibration based methodology for healing assessment. This represents a potential complementary tool to the current monitoring techniques such as CT scan, to define the appropriate time for removal of external fixation [45].

4.3.2 Vibration response with internal fixations

The capability of the vibration response technique for monitoring fracture healing of a femur treated with internal fixation has been investigated. In the work funded by the ONR, Chiu et al. [48, 49] first adopted the finite element analysis to investigate the feasibility of vibration response method with two types of internal fixation: plate–screw fixation and IM nail. The dynamic response of the femur treated with these internal fixations is quite different due to the geometry of the resulting construct. Their findings show that the healing assessment is best attempted by exploiting the bending and twisting motion of the fixated femur. As a result, they recommended a two-sensor measurement strategy (see Fig. 13). Calculating the cross-spectral function between the two sensors will allow one to determine the bending and twisting modes of the construct. The coherence function facilitated by signals from the two sensors provided assurance that the modes assessed are not unduly affected by noise.

Figure 14 shows the cross-spectrum obtained with the IM nail, which showed the sensitivity of the cross-spectrum to the state of healing. These results were condensed by Eq. (1) into the healing index and its time-derivative (see Fig. 15). These results show the viability of a non-radiative

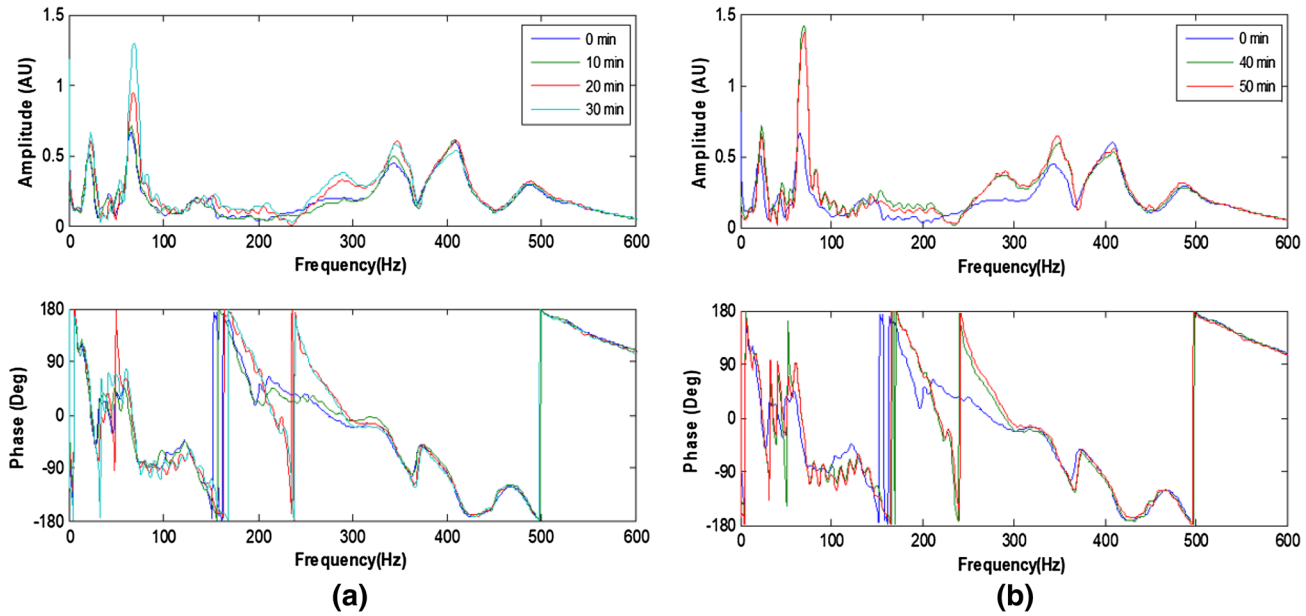

Fig. 11 Development of frequency response function resulting from simulated healing (30 min epoxy): with mass loading **a** 0–30 min; **b** 40–60 min [45]

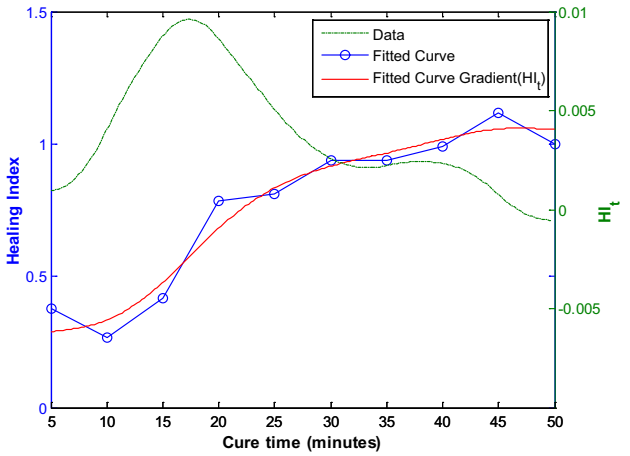

Fig. 12 Healing index calculated (with mass loading) [45]

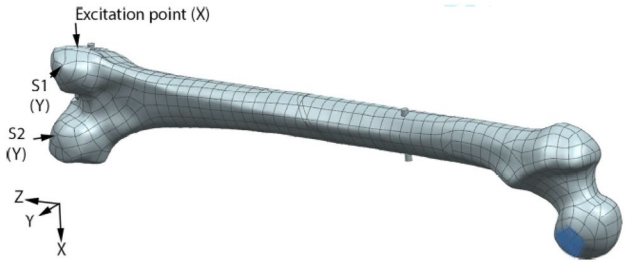

Fig. 13 Sensor placement on the numerical model and excitation point [48]

healing assessment technique based on vibration analyses. The key to this is the utilisation of the two-sensor approach that assists with the separation of the bending and the twisting modes.

Chiu et al. [50] also investigated the mass loading effect of soft tissue on the vibration-based methodology for healing assessment. The femur was wrapped with dense and highly damped plasticine to simulate soft tissue. They reported that the added mass had a minor effect on the response for the frequencies below 100 Hz. However, the change in the stiffness reflected by the spectrum was heavily hindered by the modelling clay for higher frequency modes, especially for frequency higher than 200 Hz. Figure 16 shows an example of the cross-spectrum obtained with the femur treated with IM nail. Comparing the results shown in Fig. 14, the soft-tissue effect is evident. However, the healing index derived from Fig. 16 is able to define the state of healing of the mass loaded femur. The result indicated that by using the healing index, the rate of change in the healing index and cross-spectrum could identify and monitor the fracture healing (see Fig. 17). Based on the result of Chiu et al., a concept of healing device with two transducers was established. However, a large-scale validation on accuracy and reliably of the current concept is needed for application in a clinical trial, especially the location of transducers.

5 Osseointegrated implant

Osseointegrated implant refers to a direct mechanical and functional connection between the living bone and the surface of the implant without the intervention of inter-positioned connective tissue [5, 51]. The trans-femoral osseointegrated implant (TFOI) is becoming a potential solution to replace the conventional socket device for patients who suffer from the above knee amputation [3]. Titanium alloy is widely utilised in osseointegrated implant, due to its excellent biocompatibility, superior mechanical properties and high resistance to corrosion and repeated stress loading [5, 52]. Unlike conventional socket device, TFOI is inserted into the skeletal system directly, providing better control of the prosthetic limb and improving hip joint mobility. In addition, the patients with TFOI have a fewer dermatological issue and better bone quality for the residual limb [3, 4]. Currently, there are two types of TFOI available in the market, the Osseointegrated Prostheses for Rehabilitation of Amputees (OPRA) system (Integrum AB, Göteborg, Sweden) and the implant-supported prosthesis (ISP) Endo/Exo prosthesis (Eska Implants AG, Lübeck, Germany). The OPRA system consists of a threaded titanium fixation, which is inserted into the medullary canal of the femur as illustrated in Fig. 18a. While ISP device uses a 140–180 mm slight curved titanium stem, fitting the shape of the medullary cavity, refer to Fig. 18b. Both devices include a coupling element, which protrudes through the skin, providing a connection for an artificial limb. Patients treated with TFOI required two-stage surgical procedures to achieve successful implantation. In the first stage, TFOI is inserted into the medullary canal and left unloaded for 6 to 8 weeks for the ISP system, and 3 to 6 months for the OPRA system. At the second surgery, the coupling element is attached to the distal end of fixation. Then, patients will go through a rehabilitation period in which load on the implant will gradually increase [53, 54]. It will take up to 18 months for TFOI capable of full weight load bearing.

5.1 Stability of osseointegrated implant

There are two stages of stability in the progress of osseointegration, primary and secondary. Primary stability is a mechancial stability, occured at the moment when implant inserted into bone tissue, to ensure implant is sufficient for resistance to the torsional and axial movement [5–7, 55]. For example, the primary stability provided by the interlock feature of TFOI such as the thread of OPRA and the slightly curved shape of ISP. Primary stability has been described as

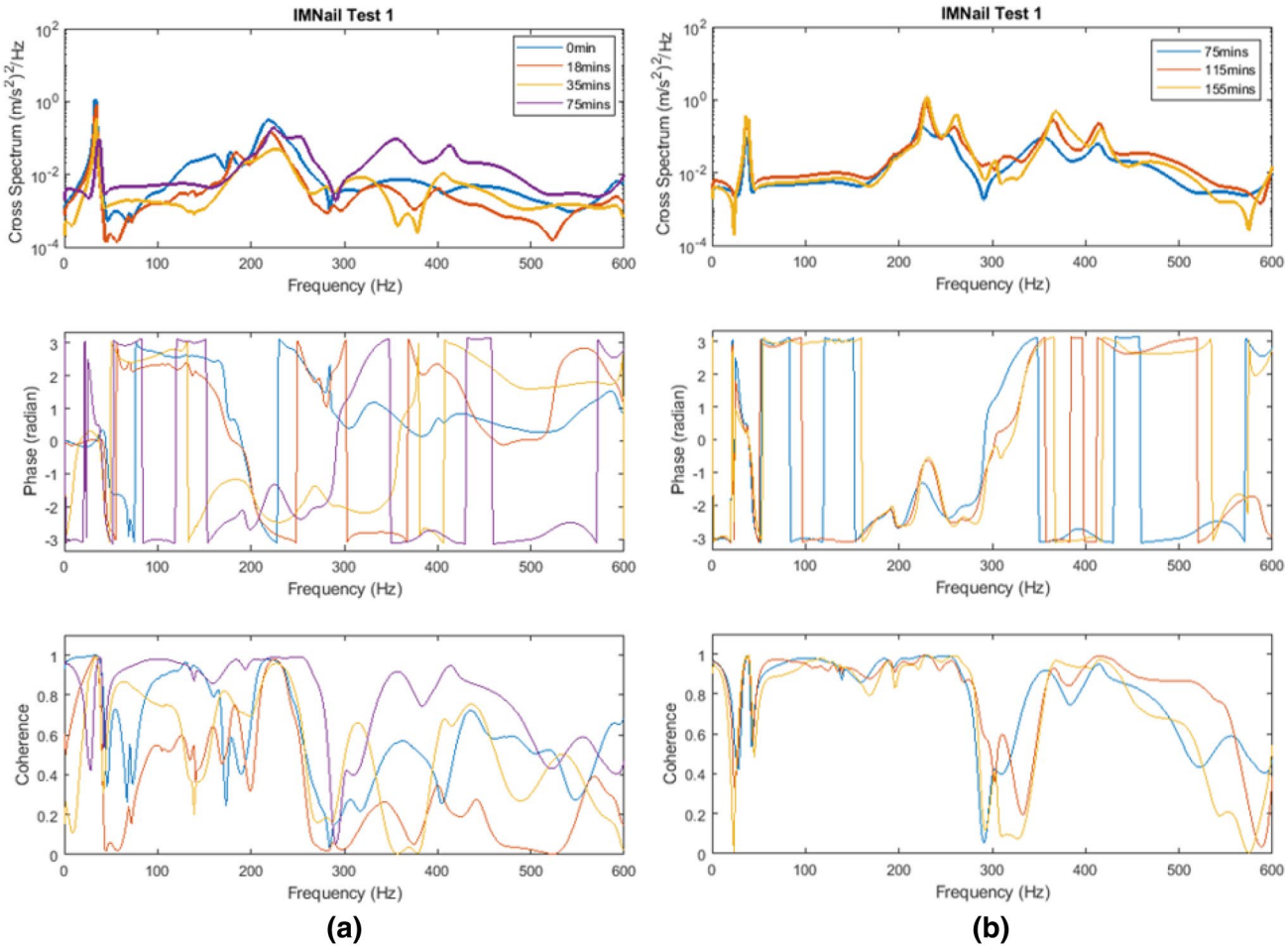

Fig. 14 Development of cross-spectrum and coherence function resulting from simulated healing (30 min epoxy) **a** 0–75 min; **b** 75–155 min. [48]

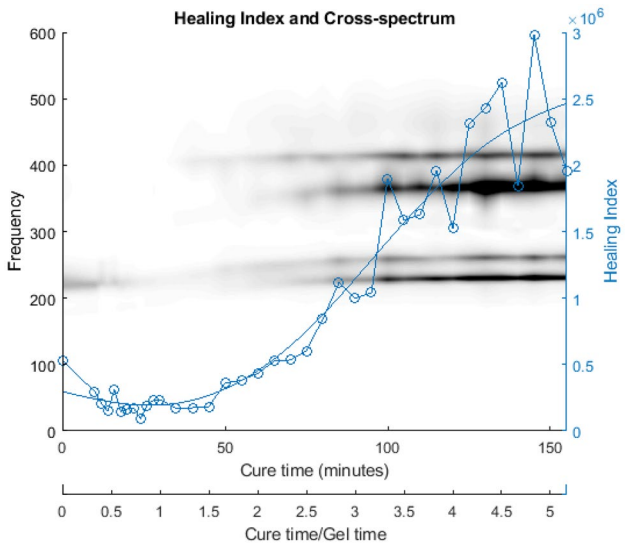

Fig. 15 Healing index calculated [48]

an important prerequisite for the long-term implant fixation not only for a hip replacement implant but also for TFOI [5–7]. In addition, based on animal experiments, Pilliar et al. [55] suggested a maximum value of 150 μm for the micro-motion between host bone and orthopaedic implant. In recent year, similar results for the hip replacement implant are exhibited in [56, 57]. Micro-motion in excess of 150 μm will compromise the structural integrity of the bone–implant system and lead to unsuccessful osseointegration to undertake load-bearing period (rehabilitation period). Moreover, insufficient primary stability will hinder the initial healing, leading to fibrous tissue formation rather than bone formation [54, 57, 58].

The secondary stability, which is the result of bone healing and remodelling, is highly reliant on the state of osseointegration [59]. Several approaches, similar to the technique of monitoring fracture healing, such as vibrational analysis, acoustic emission, and guided wave application, were proposed in a recent paper. Given that the concept of osseointegration implant originated from dentistry, the requirement

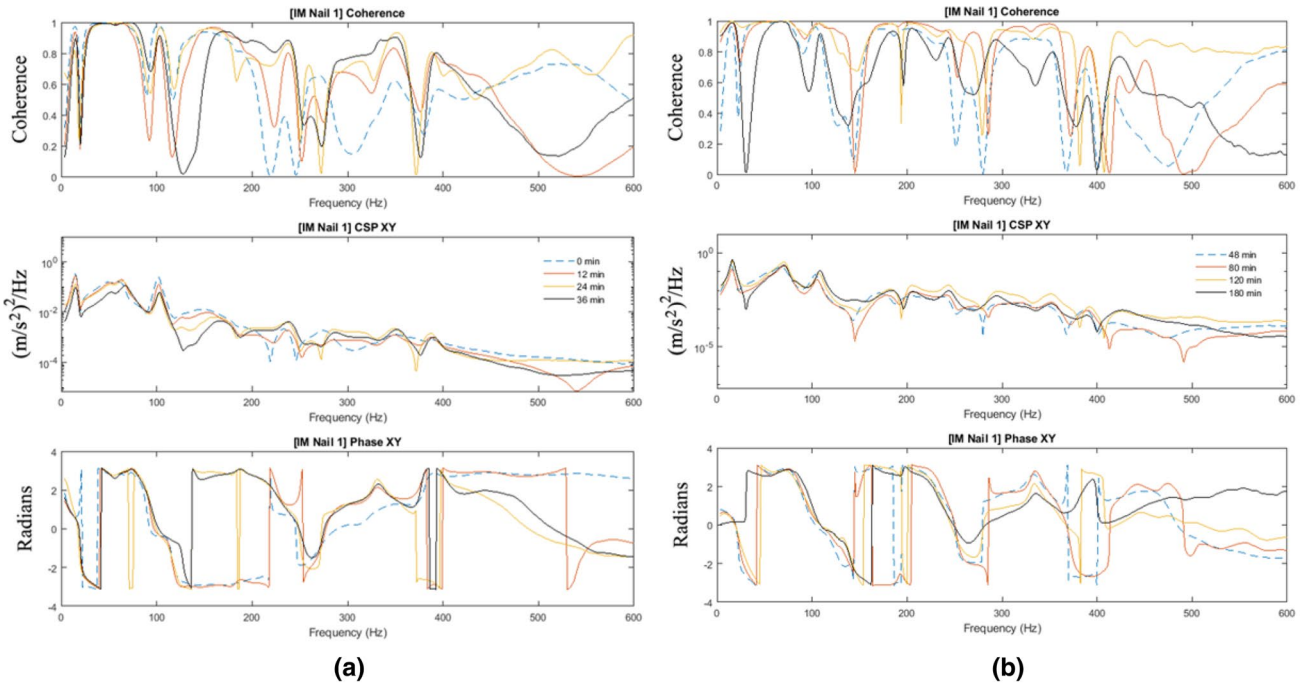

Fig. 16 Development of cross-spectrum and coherence function resulting from simulated healing (30 min epoxy) **a** 0–36 min; **b** 48–180 min [48]

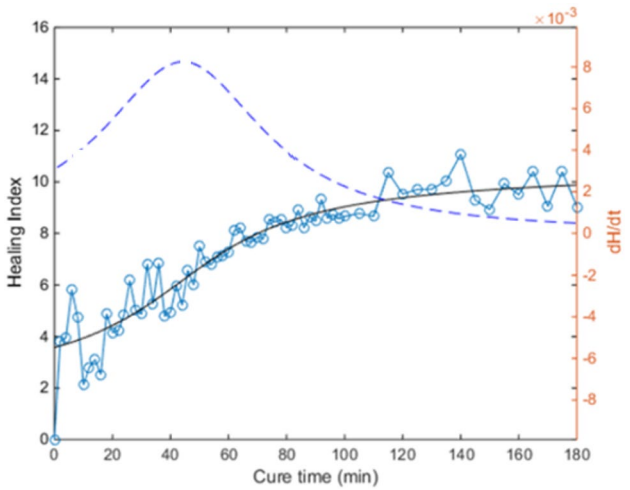

Fig. 17 Healing index [50]

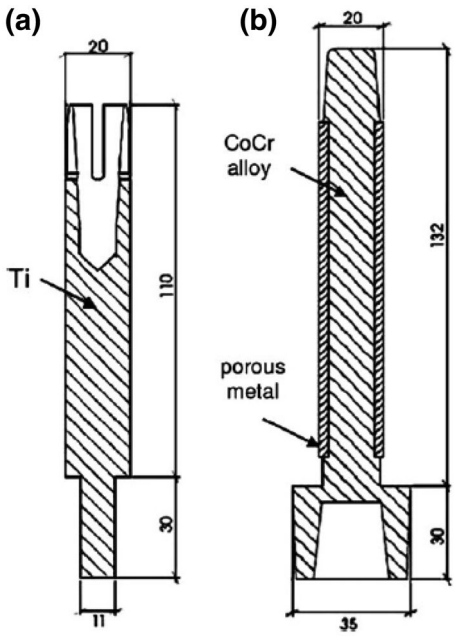

Fig. 18 Geometry of the OPRA (**a**) and ISP implant (**b**) [4]

in determining the stability of these implants has led to approaches that included the resonance frequency analysis (RFA). There are commercially available solutions such as Osstell™ ISQ and Periotest™ instruments. Osstell™ ISQ device, which transfers resonance frequency analysis value to a parameter called the implant stability quotient (ISQ), demonstrates the potential of RFA to measure the progress of osseointegration. Similar technology will be needed to assess the stability of TFOI. However, due to the structural difference such as the proportion of soft tissue and muscle constraint, there are still some limitations in applying these techniques to assessing osseointegration.

5.2 Techniques of stability assessment and monitoring for osseointegrated implants

There are different approaches to assess implant stability in vivo, such as clinical X-ray and magnetic resonance imaging (MRI). However, due to the distortion effect caused by the implant, the application of these techniques is limited [60]. The research reported in recent years evidenced the potential of quantitative assessment of osseointegration with similar techniques of monitoring fracture healing.

5.2.1 Techniques for monitoring primary stability

In the experiment on six rabbits conducted by Huang et al. [61], they investigated the relationship between resonance frequency and primary stability. They installed an implant into the predrilled cavities of 3.75 and 5 mm to simulate secure fit and loose fit condition to assess the primary stability on the left tibias of six rabbits. The result demonstrated that the loosely fitted bone–implant system had lower initial resonance frequency. In contrast, the securely fitted the bone–implant system had higher initial resonance frequency. The securely fitted bone–implant also recorded a shorter healing time. The research [62] on the hip implant stability also showed that the change in primary stability could be described by the shift in resonance frequency in the bone–implant system. In the study reported by Cairns et al. [63], they employed modal analysis to detect the change in the boundary condition of an OPRA implant. In their experiment, they applied two implant insertion torque: 4 Nm and 0.5 Nm to represent well-fitted and loose fit condition, respectively. In addition, two types of boundary condition were used: freely supported and cantilevered. Cairns et al. used an electromagnetic shaker as an excitation source. In the previous study of Carins [64], they demonstrated that the forcing provided by an electromagnetic shaker is superior to that obtained from an impact hammer in determining the resonance frequencies due to better signal-to-noise ratio. A sinusoidal sweep single with frequency ranging from 100 Hz to 10 kHz was introduced to the shaker to obtain multiple resonant frequencies of the bone–implant system. The shaker and accelerometer were attached to the distal end of the implant. Models were first tested in the Z axis and then repeated in the Y-axis refer to Fig. 19. The result exhibited that higher frequency modes, especially the second and/or third bending mode in the Z-axis, were more sensitive to the interface condition compared to the fundamental frequencies (see Fig. 20). The higher frequency modes were useful for determining the connection between bone and implant. It means that these particular modes could be the indicator of the osseointegration process. By tracking the change in these particular modes over a specified frequency range, it is possible to identify the degree of osseointegration.

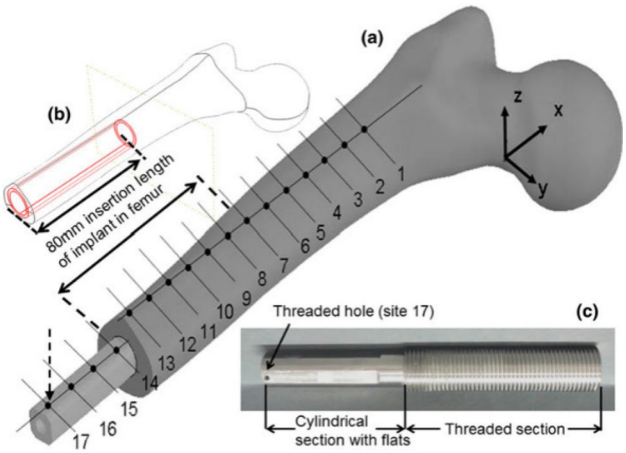

Fig. 19 Geometry of the femur–implant physical mode (**a**), insertion length of the implant in the femur (**b**) and manufactured implant (**c**) [63]

5.2.2 Techniques for monitoring secondary stability

Similar to the techniques utilizing in the monitoring of fracture healing, the potential of non-radiative methodologies is evidenced in the recent paper. Shao et al. [3] reported a study investigating the potential of using changes in the natural frequencies to assess the secondary stability of an implant (i.e. the degree of osseointegration). Authors simplified the implant as a cantilever beam, which is free to vibrate at one end and fully fixed at the other. The Natural of frequency of the beam vibration can be expressed in Eq. (2).

$$NF = \alpha \sqrt{\frac{EI}{\rho L^4}} \tag{2}$$

where L is the effective length of the beam; E is the elastic modulus; I is the moment of inertia; ρ is the vibration mass per unit length; α is a constant related to the degree of osseointegration.

The natural frequency of a mechanical or structural system (Eq. 2) is not affected by the properties of the excitation force as shown in Eq. (2). Shao et al. [3] used one accelerometer attached to the distal end of the implant to record the vibration signal (0–300 Hz). The excitation was provided by a pendulum. In their in vitro experiment, the saw-bone model was clamped at the mid-span with different silicone rubber applied on the interface between bone and implant to simulate various stages of osseointegration. The result demonstrated that the natural frequency increased as the silicone rubber layers cured (elastic modulus increases). To further investigate the state of osseointegration, they conducted nine tests during a 40-year-old male patient's rehabilitation progress. According to the result, a reduction of natural frequency was detected after the first weight bearing,

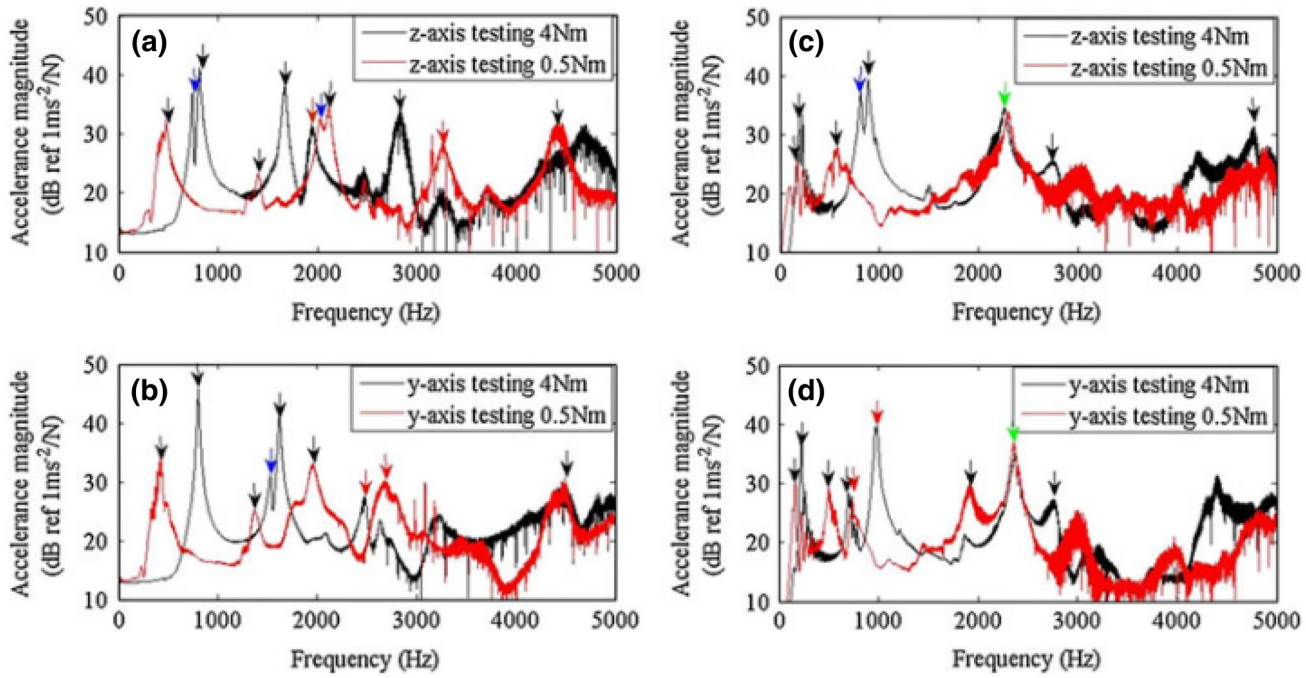

Fig. 20 Mean accelerance functions for the freely supported models (**a**, **b**), and cantilevered models (**c**, **d**). The green arrows indicate resonance seen in both 4 Nm and 0.5 Nm models; red arrows indicate the repeated second bending; black arrows indicate other resonant frequencies; blue arrows indicate a component of resonance from the orthogonal axis (colour figure online) [63]

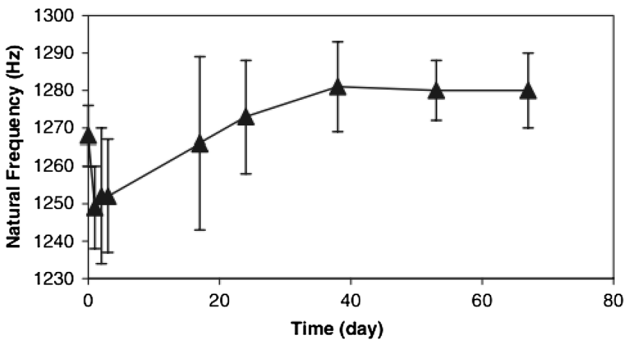

Fig. 21 In-vivo NF measurements during the weight-bearing rehabilitation [3]

Table 1 Mean value ± SD of the evaluated central frequencies cf over 4 weeks [65]

Measurement	Central frequency (kHz)
m0	7.14 ± 3.29
m1	6.01 ± 3.73
m2	7.39 ± 3.35
m3	10.59 ± 2.85
m4	13.56 ± 2.52

which indicated the lack of osseointegration (see Fig. 21). Following that event, the natural frequency measured was reported to increase gradually until the patient was capable of bearing his full weight load. They concluded that there is a clear correlation between the value of natural frequency and load-bearing ability of the patient. A similar result was also reported in an animal experiment [61] that the resonance frequency increased significantly during the healing period and peaked when the implant was united with bone.

Beside technique of employing natural frequency as indicator to measure the secondary stability, Ruther et al. [65]. reported on a novel acoustic method in their attempt to investigate the correlation between the frequency spectrum of the recorded acoustic sound and the pulled-out strength. In their work, a magnetic sphere was placed in a hollow cylinder implant. An external magnetic field was used to excite the sphere as an acoustic source. They conducted an experiment on 20 rabbits with a specially designed implant inserted and excited within the frequency band of 0 to 28 kHz. The acoustic analysis was performed each week (denoted as m0 to m4). The result shown in Table 1 demonstrated that the central frequency decreased in the first week, followed by a significant increase until full osseointegration. Given that the acoustic pattern of an implant highly depended on several parameters such as bone dimension, implant position, and distant to the measurement location, making it difficult to conclude a standard of successful osseointegration.

Similar to the technique used to monitor the fracture healing process, guided wave (GW) method has significant potential to assess implant stability [66, 69, 71]. GW method was firstly applied in evaluated the stability of the dental implant, and recently, this technique was also employed as a monitoring tool for the stability of osseointegrated implant [66–69]. Due to the similar process occurred at the bone–implant interface, the verdict obtained from dental implant could provide a foundation for the development of GW application in osseointegrated implant. In recent research, Wang and Lynch [66] reported an application of the guided wave on assessing the degree of osseointegration of OPRA system. In their report, they used Gaussian process regression to analyse the energy of reflected guided wave (longitudinal wave mode) relative to the state of osseointegration. They applied epoxy, which has 30-min curing time to the interface of bone and implant to simulate the osseointegration process. According to the result of finite element analysis and in vitro experiment, the trend of energy variation was similar to the result of dental implant reported in [60]. Their work demonstrated that the energy of the reflected wave decreased in the first 30 min (epoxy curing). The energy plateaued when the epoxy was solidified. In addition, the energy increased significantly after the "pull-out" of an implant. These findings revealed that the energy of the longitudinal wave mode was sensitive to the change of interface condition and the capability of the GW method in evaluating the degree of osseointegration. Similar influences were also reported in the works on dental implant reported in [67, 68]. These result provided a general basis for the development of guided wave application in monitoring implant stability.

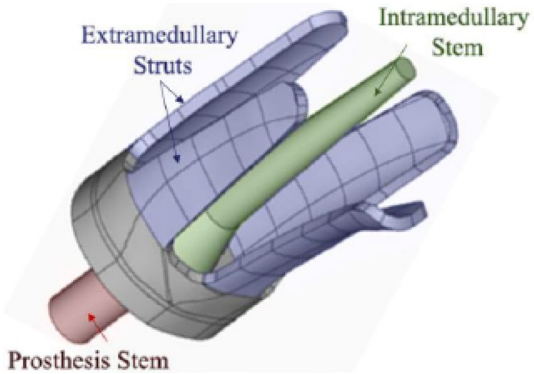

Fig. 22 The customizable OI design proposed by Russ et al. [70]

Recently, in the research funded by ONR, Vien et al. [69] reported on a GW methodology to monitor the state of osseointegration by incorporating embedded sensors on a novel implant. The system was based on a customisable osseointegrated implants proposed by Russ et al. [70] (see Fig. 22). Given that the cross-sectional shapes varied with anatomic location along a femur, two types of cross-section were investigated: oval and triangular (see Fig. 23). The actuator, which bonded to extramedullary struts, excited a 1 MHz triangular pulse signal. Two transducers were employed in this experiment refer to Fig. 23. Adhesive epoxy was applied to the bone–implant interface to simulate the osseointegration process. The core of specimens was filled with silicone to simulation soft spongy bone in the medullary cavity, and plasticine was applied to the around the whole specimen to investigate the damping effect caused by soft tissue. According to the result of previous FE simulation [71], a circumferential wave mode was expected to propagate on both the oval and triangular cross-section implant.

Vien et al. introduced an osseointegration index (O-Index) as shown in Eq. (3). The healing index compared the energy of the signal transmitted from the actuator to the sensor to baseline energy as a function of time. According to the result, the frequency band of 130 to 250 kHz was the most sensitive to the curing of the epoxy. In addition, the O-Index demonstrated a clear increasing asymptotic trend relative to the curing time for both oval and triangular implant, excepting the near case for the triangular specimen (see Fig. 24). It is evident that the

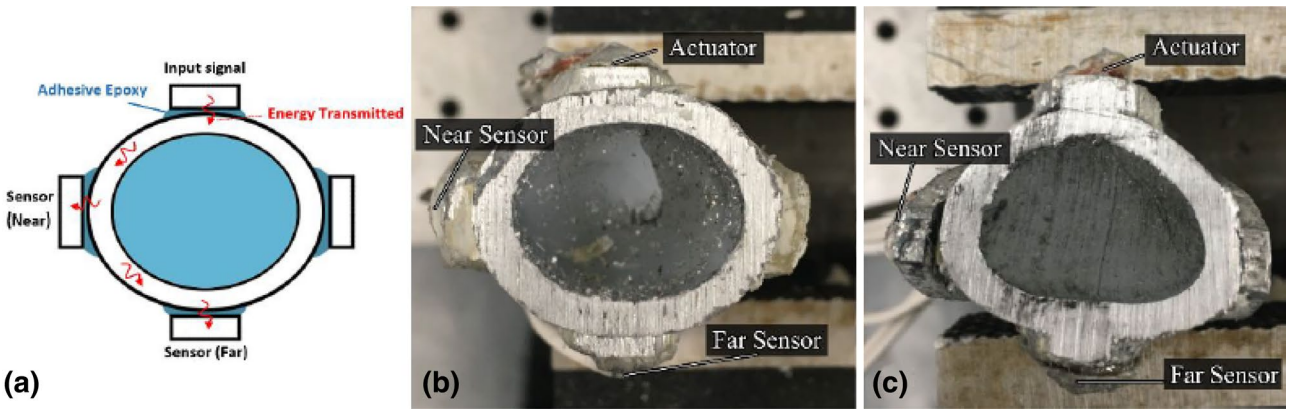

Fig. 23 **a** Sensors location, **b** oval and **c** triangular-like specimens filled with silicone [69]

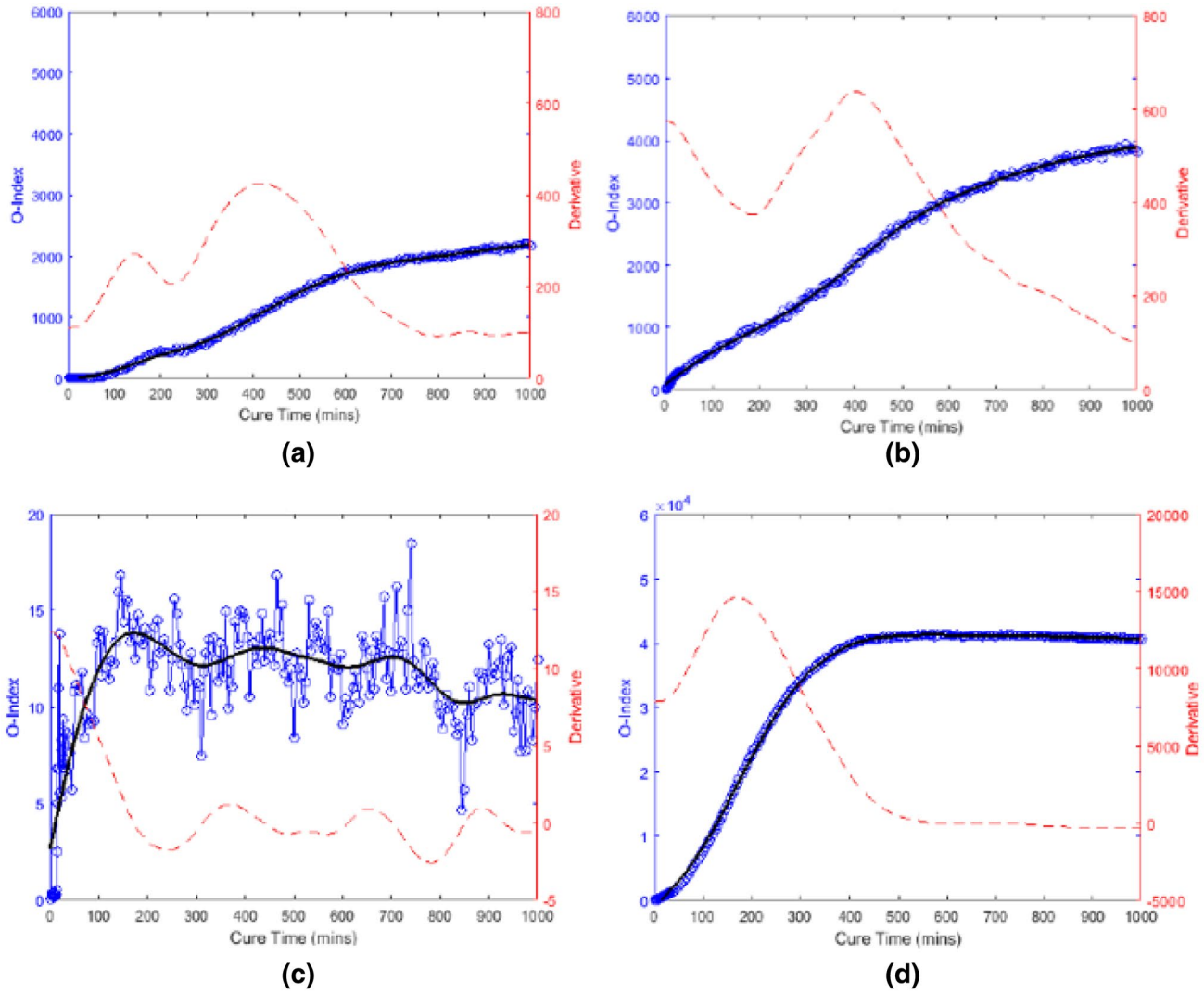

Fig. 24 O-Index with its time derivative for **a** Oval specimen (near); **b** Oval specimen (far); **c** Triangular specimen (near); **d** Triangular specimen (far) [69]

damping effect caused by the silicone and plasticine had no effect on O-Index and the ability of O-Index on evaluating the degree of osseointegration. At the conclusion of the experiment, researchers removed the plasticine and noted that the result in Fig. 24c is attributed to the fact that the extramedullary strut was not fully bonded with the bone model. They showed that the O-Index is capable of assessing the progression of osseointegration, the achievement of complete osseointegration and, equally as important, the lack of osseointegration. However, the major barrier to its transition into the clinical and research practice is the shortage of research on diagnostic accuracy and reliability for various types of bone cross-section. In addition, the effect of soft tissue requires further investigation in the in vivo condition.

$$
\begin{aligned}
g(T,t) &= g\left(T_i,t\right) - g\left(T_0,t\right) \\
G(T,f) &= \int_{-\infty}^{\infty} g(T,t)e^{-i2\pi ft}dt \\
G_0(f) &= \int_{-\infty}^{\infty} g\left(T_0,t\right)e^{-i2\pi ft}dt \\
Osseontegration\ index\ \left(T=T_i\right) &\propto \int_{f_1}^{f_2} \frac{|G(T,f)|^2}{|G_0(f)|^2}df
\end{aligned}
\tag{3}
$$

where $g(T_i, t)$ is the time signal at any cure time; $g(T_0, t)$ is the time signal (baseline signal) at initial cure time $T_0 = 0$ min; $g(T, t)$ is the difference in time signal relative to initial cure time; $G_0(f)$ is the Fourier Transform of the baseline signal; $G(T, f)$ is the Fourier Transform of difference in cure time signal; $(T_i \neq T_0)$.

6 Conclusion

This paper reviewed works pertaining to the fracture healing assessment techniques that have been reported on. Particular emphasised is placed on the non-radiative techniques that utilises the dynamic response of a fixated long bone to determine the state of healing. The review also provide an overview of the development and monitoring of osseointegrated implants. TFOI, which improves joint mobility and bone quality, was proposed in recent year as a replacement treatment for the patient with a socket device. However, excessive micro-movement at the bone–implant interface leads to a failure osseointegration formation.

The review showed that there is a common thread between the healing assessment of a fixated long bone and the need to determine the primary and secondary stability of osseointegrated implants. It is evident that the potential of a dynamics-based methodology for quantitative assessment is real. However, large-scale validation on repeatability and accuracy of the results is needed. From the works reviewed, there is a good prospect of further developing the following non-radiative assessment tools:

a. Low-frequency vibration based technique for healing assessment of long bones and the primary stability of osseointegrated implants.
b. High-frequency acousto-ultrasonic based methodology for assessing the secondary stability of osseointegrated implants.

Funding This research is funded by US Navy Office of Naval Research (N00014-18-1-2336). The financial supported provided by the Office of Naval Research is gratefully acknowledged.

Compliance with ethical standards

Conflict of interest The author declares that there is no conflict of interest regarding the publication of this paper.

Ethical approval This article does not contain any studies with human participants or animals performed by any of the authors.

References

1. Claes L, Cunningham J. Monitoring the mechanical properties of healing bone. Clin Orthop Relat Res. 2009;467(8):1964–71. https://doi.org/10.1007/s11999-009-0752-7.
2. Morshed S, Corrales L, Genant H, Miclau T. Outcome assessment in clinical trials of fracture-healing. J Bone Joint Surg Am. 2008;90(1):62–7. https://doi.org/10.2106/jbjs.g.01556.
3. Shao F, Xu W, Crocombe A, Ewins D. Natural frequency analysis of osseointegration for trans-femoral implant. Ann Biomed Eng. 2007;35(5):817–24. https://doi.org/10.1007/s10439-007-9276-z.
4. Tomaszewski P, Verdonschot N, Bulstra S, Verkerke G. A comparative finite-element analysis of bone failure and load transfer of osseointegrated prostheses fixations. Ann Biomed Eng. 2010;38(7):2418–27. https://doi.org/10.1007/s10439-010-9966-9.
5. Isaacson B, Jeyapalina S. Osseointegration: a review of the fundamentals for assuring cementless skeletal fixation. Orthop Res Rev. 2014. https://doi.org/10.2147/orr.s59274.
6. Bieger R, Ignatius A, Decking R, Claes L, Reichel H, Dürselen L. Primary stability and strain distribution of cementless hip stems as a function of implant design. Clin Biomech. 2012;27(2):158–64. https://doi.org/10.1016/j.clinbiomech.2011.08.004.
7. Morelli F, Lang N, Bengazi F, Baffone D, Dadonim Vila Morales C, Botticelli D. Influence of bone marrow on osseointegration in long bones: an experimental study in sheep. Clin Oral Implant Res. 2014;26(3):300–6. https://doi.org/10.1111/clr.12487.
8. Harwood P, Ferguson D. (ii) An update on fracture healing and non-union. Orthop Trauma. 2015;29(4):228–42. https://doi.org/10.1016/j.mporth.2015.07.004.
9. Marsell R, Einhorn T. The biology of fracture healing. Injury. 2011;42(6):551–5. https://doi.org/10.1016/j.injury.2011.03.031.
10. Mora-Macías J, Reina-Romo E, López-Pliego M, Giráldez-Sánchez M, Domínguez J. In vivo mechanical characterization of the distraction callus during bone consolidation. Ann Biomed Eng. 2015;43(11):2663–74. https://doi.org/10.1007/s10439-015-1330-7.
11. Leong P, Morgan E. Measurement of fracture callus material properties via nanoindentation. Acta Biomater. 2008;4(5):1569–75. https://doi.org/10.1016/j.actbio.2008.02.030.
12. Leong P, Morgan E. Correlations between indentation modulus and mineral density in bone-fracture calluses. Integr Comp Biol. 2009;49(1):59–68. https://doi.org/10.1093/icb/icp024.
13. Dwyer J, Owen P, Evans G, Kuiper J, Richardson J. Stiffness measurements to assess healing during leg lengthening. J Bone Joint Surg Br. 1996;78(2):286–9. https://doi.org/10.1302/0301-620x.78b2.0780286.
14. Chehade M, Pohl A, Pearcy M, Nawana N. Clinical implications of stiffness and strength changes in fracture healing. J Bone Joint Surg. 1997;79(1):9–12. https://doi.org/10.1302/0301-620x.79b1.6324.
15. Moss DP, Tejwani NC. Biomechanics of external fixation. Bull NYU Hosp Jt Dis. 2007;65(4):294–9.
16. Green SA. Complications of external skeletal fixation. Clin Orthop Relat Res. 1983;180:109–16.
17. Perren S. Evolution of the internal fixation of long bone fractures. J Bone Joint Surg Br. 2002;84(8):1093–110. https://doi.org/10.1302/0301-620x.84b8.0841093.
18. Eveleigh R. A review of biomechanical studies of intramedullary nails. Med Eng Phys. 1995;17(5):323–31. https://doi.org/10.1016/1350-4533(95)97311-c.
19. Parekh A, et al. Treatment of distal femur and proximal tibia fractures with external fixation followed by planned conversion to internal fixation. J Trauma. 2008;64(3):736–9. https://doi.org/10.1097/ta.0b013e31804d492b.

20. Miller D, Goswami T. A review of locking compression plate biomechanics and their advantages as internal fixators in fracture healing. Clin Biomech. 2007;22(10):1049–62. https://doi.org/10.1016/j.clinbiomech.2007.08.004.
21. Thapa N, Prayson M, Goswami T. A failure study of a locking compression plate implant. Case Stud Eng Fail Anal. 2015;3:68–72. https://doi.org/10.1016/j.csefa.2015.03.004.
22. Chiu W, Vien B, Russ M, Fitzgerald M. Towards a non-invasive technique for healing assessment of internally fixated femur. Sensors. 2019;19(4):857. https://doi.org/10.3390/s19040857.
23. Benirschke S, Mirels H, Jones D, Tencer A. The use of resonant frequency measurements for the noninvasive assessment of mechanical stiffness of the healing tibia. J Orthop Trauma. 1993;7(1):64–71. https://doi.org/10.1097/00005131-199302000-00012.
24. den Boer F, et al. Quantification of fracture healing with three-dimensional computed tomography. Arch Orthop Trauma Surg. 1998;117(6–7):345–50. https://doi.org/10.1007/s004020050263.
25. Sigurdsen U, Reikeras O, Hoiseth A, Utvag S. Correlations between strength and quantitative computed tomography measurement of callus mineralization in experimental tibial fractures. Clin Biomech. 2011;26(1):95–100. https://doi.org/10.1016/j.clinbiomech.2010.09.004.
26. Lamy F, Takarli M, Angellier N, Dubois F, Pop O. Acoustic emission technique for fracture analysis in wood materials. Int J Fract. 2015;192(1):57–70. https://doi.org/10.1007/s10704-014-9985-x.
27. Prosser WH, Allison SG, Woodard SE, Wincheski RA, Cooper EG, Price DC, Hedley M, Prokopenko M, Scott DA, Tessler A. Structural health management for future aerospace vehicles. 2004.
28. Prosser WH, Gorman MR, Madaras EI. Acoustic emission detection of impact damage on space shuttle structures. 2004.
29. Hirasawa Y, Takai S, Kim W, Takenaka N, Yoshino N, Watanabe Y. Biomechanical monitoring of healing bone based on acoustic emission technology. Clin Orthop Relat Res. 2002;402:236–44. https://doi.org/10.1097/00003086-200209000-00023.
30. Shrivastava S. Assessment of bone condition by acoustic emission technique: a review. J Biomed Sci Eng. 2009;02(03):144–54. https://doi.org/10.4236/jbise.2009.23025.
31. Agcaoglu S, Akkus O. Acoustic emission based monitoring of the microdamage evolution during fatigue of human cortical bone. J Biomech Eng. 2013;135(8):081005. https://doi.org/10.1115/1.4024134.
32. Watanabe Y, Takai S, Arai Y, Yoshino N, Hirasawa Y. Prediction of mechanical properties of healing fractures using acoustic emission. J Orthop Res. 2001;19(4):548–53. https://doi.org/10.1016/s0736-0266(00)00042-5.
33. Protopappas V, Vavva M, Fotiadis D, Malizos K. Ultrasonic monitoring of bone fracture healing. IEEE Trans Ultrason Ferroelectr Freq Control. 2008;55(6):1243–55. https://doi.org/10.1109/tuffc.2008.787.
34. Abendschein W, Hyatt G. Ultrasonics and physical properties of healing bone. J Trauma. 1972;12(4):297–301. https://doi.org/10.1097/00005373-197204000-00005.
35. Gerlanc M, Haddad D, Hyatt G, Langloh J, St. Hilaire P. Ultrasonic study of normal and fractured bone. Clin Orthop Relat Res. 1975;111:175–80. https://doi.org/10.1097/00003086-197509000-00025.
36. Vavva MG, Protopappas VC, Fotiadis DI, Malizos KN. Ultrasound velocity measurements on healing bones using the external fixation pins: a two-dimensional simulation study. J Serb Soc Comput Mech. 2008;2(2):1–15.
37. Malizos K, Papachristos A, Protopappas V, Fotiadis D. Transosseous application of low-intensity ultrasound for the enhancement and monitoring of fracture healing process in a sheep osteotomy model. Bone. 2006;38(4):530–9. https://doi.org/10.1016/j.bone.2005.10.012.
38. Protopappas V, Fotiadis D, Malizos K. Guided ultrasound wave propagation in intact and healing long bones. Ultrasound Med Biol. 2006;32(5):693–708. https://doi.org/10.1016/j.ultrasmedbio.2006.02.001.
39. Tatarinov A, Sarvazyan N, Sarvazyan A. Use of multiple acoustic wave modes for assessment of long bones: model study. Ultrasonics. 2005;43(8):672–80. https://doi.org/10.1016/j.ultras.2005.03.004.
40. Di Puccio F, Mattei L, Longo A, Marchetti S. Investigation on the feasibility of bone stiffness assessment from in-vivo tests. In: XXIII conference of the Italian Association of theoretical and applied mechanics; 2017. vol. 2, pp. 594–601.
41. Alizad A, Walch M, Greenleaf J, Fatemi M. Vibrational characteristics of bone fracture and fracture repair: application to excised rat femur. J Biomech Eng. 2006;128(3):300. https://doi.org/10.1115/1.2187037.
42. Tower S, Beals R, Duwelius P. Resonant frequency analysis of the tibia as a measure of fracture healing. J Orthop Trauma. 1993;7(2):179. https://doi.org/10.1097/00005131-199304000-00063.
43. Bediz B, Nevzat Özgüven H, Korkusuz F. Vibration measurements predict the mechanical properties of human tibia. Clin Biomech. 2010;25(4):365–71. https://doi.org/10.1016/j.clinbiomech.2010.01.002.
44. Ong W, Chiu W, Russ M, Chiu Z. Extending structural health monitoring concepts for bone healing assessment. Fatigue Fract Eng Mater Struct. 2016;39(4):491–501. https://doi.org/10.1111/ffe.12382.
45. Ong W, Chiu W, Russ M, Chiu Z. Integrating sensing elements on external fixators for healing assessment of fractured femur. Struct Control Health Monit. 2016;23(12):1388–404. https://doi.org/10.1002/stc.1843.
46. Mattei L, Longo A, Di Puccio F, Ciulli E, Marchetti S. Vibration testing procedures for bone stiffness assessment in fractures treated with external fixation. Ann Biomed Eng. 2016;45(4):1111–21. https://doi.org/10.1007/s10439-016-1769-1.
47. Nakatsuchi Y, Tsuchikane A, Nomura A. The vibrational mode of the tibia and assessment of bone union in experimental fracture healing using the impulse response method. Med Eng Phys. 1996;18(7):575–83. https://doi.org/10.1016/1350-4533(96)00010-0.
48. Chiu W, Vien B, Russ M, Fitzgerald M. Vibration-based healing assessment of an internally fixated femur. J Nondestr Eval Diagn Progn Eng Syst. 2019. https://doi.org/10.1115/1.4043276.
49. Chiu W, Ong W, Russ M, Fitzgerald M. Simulated vibrational analysis of internally fixated femur to monitor healing at various fracture angles. Procedia Eng. 2017;188:408–14. https://doi.org/10.1016/j.proeng.2017.04.502.
50. Chiu W, Vien B, Russ M, Fitzgerald M. Healing assessment of fractured femur treated with an intramedullary nail. Struct Health Monit. 2019. https://doi.org/10.1177/1475921718816781.
51. Branemark R, Branemark PI, Rydevik B, Myers RR. Osseointegration in skeletal reconstruction and rehabilitation. J Rehabil Res Dev. 2001;38:175–81.
52. Agarwal R, García A. Biomaterial strategies for engineering implants for enhanced osseointegration and bone repair. Adv Drug Deliv Rev. 2015;94:53–62. https://doi.org/10.1016/j.addr.2015.03.013.
53. Gallagher P, Desmond D, MacLachlan M. Psychoprosthetics. London: Springer; 2008. p. 131–40.
54. Ward DA, Robinson KP. Osseointegration for the skeletal fixation of limb prostheses in amputations at the trans-femoral level. In: Brånemark P-I, editor. The osseointegration book. Berlin: Quintessenz Verlags; 2005. p. 463–76.

55. Pilliar R, Lee J, Maniatopoulos C. Observations on the effect of movement on bone ingrowth into porous-surfaced implants. Clin Orthop Relat Res. 1986;7(208):108–13. https://doi.org/10.1097/00003086-198607000-00023.
56. Bieger R, Ignatius A, Reichel H, Dürselen L. Biomechanics of a short stem: in vitro primary stability and stress shielding of a conservative cementless hip stem. J Orthop Res. 2013;31(8):1180–6. https://doi.org/10.1002/jor.22349.
57. Østbyhaug P, Klaksvik J, Romundstad P, Aamodt A. Primary stability of custom and anatomical uncemented femoral stems. Clin Biomech. 2010;25(4):318–24. https://doi.org/10.1016/j.clinbiomech.2009.12.012.
58. Lioubavina-Hack N, Lang N, Karring T. Significance of primary stability for osseointegration of dental implants. Clin Oral Implant Res. 2006;17(3):244–50. https://doi.org/10.1111/j.1600-0501.2005.01201.x.
59. Isaacson B, Vance R, Rosenbaum Chou T, Bloebaum R, Bachus K, Webster J. Effectiveness of resonance frequency in predicting orthopedic implant strength and stability in an in vitro osseointegration model. J Rehabil Res Dev. 2009;46(9):1109. https://doi.org/10.1682/jrrd.2009.06.0080.
60. Vayron R, Soffer E, Anagnostou F, Haïat G. Ultrasonic evaluation of dental implant osseointegration. J Biomech. 2014;47(14):3562–8.
61. Huang H, Chiu C, Yeh C, Lin C, Lin L, Lee S. Early detection of implant healing process using resonance frequency analysis. Clin Oral Implant Res. 2003;14(4):437–43. https://doi.org/10.1034/j.1600-0501.2003.00818.x.
62. Lannocca M, Varini E, Cappello A, Cristofolini L, Bialoblocka E. Intra-operative evaluation of cementless hip implant stability: a prototype device based on vibration analysis. Med Eng Phys. 2007;29(8):886–94. https://doi.org/10.1016/j.medengphy.2006.09.011.
63. Cairns N, Pearcy M, Smeathers J, Adam C. Ability of modal analysis to detect osseointegration of implants in transfemoral amputees: a physical model study. Med Biol Eng Comput. 2012;51(1–2):39–47. https://doi.org/10.1007/s11517-012-0962-0.
64. Cairns NJ, Adam CJ, Pearcy MJ, Smeathers J. Evaluation of modal analysis techniques using physical models to detect osseointegration of implants in transfemoral amputees. In: Patton J, editor. Engineering in medicine and biology society (EMBC), 2011 annual international conference of the IEEE, Boston, USA; 2011. pp. 1600–1603.
65. Ruther C, et al. In vivo monitoring of implant osseointegration in a rabbit model using acoustic sound analysis. J Orthop Res. 2014;32(4):606–12. https://doi.org/10.1002/jor.22574.
66. Wang W, Lynch J. IWSHM 2017: application of guided wave methods to quantitatively assess healing in osseointegrated prostheses. Struct Health Monit. 2018;17(6):1377–92. https://doi.org/10.1177/1475921718782399.
67. Vayron R, Mathieu V, Michel A, Haïat G. Assessment of in vitro dental implant primary stability using an ultrasonic method. Ultrasound Med Biol. 2014;40(12):2885–94. https://doi.org/10.1016/j.ultrasmedbio.2014.03.035.
68. Mathieu V, Vayron R, Soffer E, Anagnostou F, Haïat G. Influence of healing time on the ultrasonic response of the bone–implant interface. Ultrasound Med Biol. 2012;38(4):611–8. https://doi.org/10.1016/j.ultrasmedbio.2011.12.014.
69. Vien B, Chiu W, Russ M, Fitzgerald M. A quantitative approach for the bone–implant osseointegration assessment based on ultrasonic elastic guided waves. Sensors. 2019;19(3):454. https://doi.org/10.3390/s19030454.
70. Russ M, Chiu W, Ong HW, Tran T, Russ M, Fitzgerald M. Development of a novel osseointegrated endoprosthesis, combing orthopaedic and engineering design principles, and structural health monitoring conc. Struct Health Monit. 2017. https://doi.org/10.12783/shm2017/14244.
71. Vien B, Chiu W, Russ M, Fitzgerald M. A stress wave-based health monitoring concept on a novel osseointegrated endoprosthesis design. In: 7th Asia-Pacific workshop on structural health monitoring (APWSHM); 2018.